# MAGNETIC LOCAL TIME SURVEY OF RADIATION BELT HELIUM ION STRUCTURE CONDUCTED WITH DATA FROM THE POLAR CAMMICE/HIT INSTRUMENT

W. N. Spjeldvik* and T. A. Fritz, R. B. Sheldon and J. Chen

Center for Space Physics, Boston University, Boston, MA 02215, USA

Camera-ready Copy for

**Paros Conference**

Manuscript-No. 12345

**Offset requests to:**
W. N. Spjeldvik
Weber State University
Ogden, UTAH

*also at Physics Dept., Weber State University, Ogden, UT 84408-2508, USA

# MAGNETIC LOCAL TIME SURVEY OF RADIATION BELT HELIUM ION STRUCTURE CONDUCTED WITH DATA FROM THE POLAR CAMMICE/HIT INSTRUMENT

**W. N. Spjeldvik*** **and T. A. Fritz, R. B. Sheldon and J. Chen**
Center for Space Physics, Boston University, Boston, MA 02215, USA
*also at Physics Dept., Weber State University, Ogden, UT 84408-2508, USA

Received 1 January 1998 – Accepted 1 March 1998

**Abstract.** A study of geomagnetically confined helium ions in the range 0.52–8.2 MeV ion kinetic energy was made with the CAMMICE Heavy Ion Telescope (HIT) during April–October 1996. Much of the year 1996 was remarkably geomagnetically quiescent with absence of major magnetic storms, large shock transits through the magnetosphere, or penetration injection events. Indeed, between two minor magnetic "storms" on January 13 ($D_{ST}$ minimum $\sim$ -88 nT) and October 23 ($D_{ST}$ minimum $\sim$ -110 nT) 1996 there was a long geomagnetically relatively undisturbed time period with $D_{ST}$ excursions in the few tens of nT at most. Using the POLAR ephemeris data, it was found that the nominal $L$-parameter location of the radial peaks in helium ion fluxes varied considerably with azimuthal location around the Earth, i.e., with magnetic local time (MLT), to be observed at $L$=2.7–2.6 respectively in the dawn sector (near MLT$\sim$5 hr) and typically a nominal $L$-parameter farther out in the dusk sector (near MLT$\sim$17 hr). The empirical helium ion anisotropy could be reasonably approximated by an unambiguous $\sin^n \alpha_0$ dependence (where $\alpha_0$ is equatorial pitch angle) only fairly close to the geomagnetic equator, at equatorial pitch angles $\alpha_0 > 45°$. For smaller equatorial pitch angles, the distribution was often seen to be flatter than describable by this relation alone. There may be several interacting causes of these observed features, including (1) effects of differences between the real geomagnetic field and the model field (IGRF 95) used in the POLAR ephemeris, (2) consequences of coupling between ion transport dynamics, spectra and exospheric interactions, and (3) possibly also real physical effects of the azimuthally asymmetric geoelectric field in conjunction with large gradients in the helium ion distribution function. Further work is needed to delineate the relative importance of these influences on the structure of radiation belt helium ions.

*Correspondence to:* W. N. Spjeldvik

## 1 Introduction

Over the preceding decades there have been several studies of geomagnetically trapped energetic helium ions (e.g., Chen et al., 1994, 1996; Cornwall, 1972; Fritz and Spjeldvik, 1978, 1979, 1982; Krimigis and Van Allen, 1976; Lemaire, 1996; Panasyuk and Vlasova, 1981; Pugacheva et al., 1996; Reeves, 1996; Sheldon and Hamilton, 1993; Spjeldvik and Fritz, 1978, 1981, 1983; Tverskoy, 1971, and others). From these works we have obtained valuable data on the radial structure and spectral characteristics on MeV helium ions, and there have been theoretical and experimental summaries (e.g., Schulz and Lanzerotti, 1974; Spjeldvik, 1979; Spjeldvik and Rothwell, 1985). For radiation belt protons, there exist empirical models compiled by NASA as well as a survey of proton pitch angle anisotropies with local time, energy and $L$-shell (e.g., Garcia and Spjeldvik, 1985). But for radiation belt helium ions, detailed data to carry out a local time variation assessment have until now not been available.

As a part of the International Solar Terrestrial Physics (ISTP) and Global Geophysics Study (GGS) Programs, the POLAR spacecraft was launched on February 24, 1996 from Vandenberg Air Force Base in California and achieved a polar orbit with perigee below 2 earth radii over the Earth's south pole and apogee above 8 earth radii over the north pole. The spacecraft spins on a time scale of six seconds with a spacecraft spin axis orientation such that instruments with pointing direction perpendicular to the spin axis nominally samples all directions to the geomagnetic field in each spin as POLAR crosses the geomagnetic equatorial plane.

Amongst the extensive instrumentation on the POLAR spacecraft is the CAMMICE instrument package which contains the Heavy Ion Telescope (HIT) consisting of a stack of solid state detectors. It is mounted

**Table 1.** CAMMICE/HIT Helium Ion Channels

| Passband ID | Energy Passband Range in MeV | Particle Species |
|---|---|---|
| HID-5 | 0.52 – 1.15 | Helium + pile-up $H^+$ |
| HID-6 | 1.15 – 1.80 | Helium |
| HID-7 | 1.80 – 2.40 | Helium |
| HID-8 | 2.40 – 8.20 | Helium |

perpendicular to the spacecraft spin axis, and it is operating with a temporal resolution of 16 sector samples per spin period (i.e., with an angular sampling resolution of 22.5°) and an aperture opening angle of ±8°. We here report observations of geomagnetically trapped helium ions in four energy ranges from 0.52–8.2 MeV. These are specified in Table 1. The geometric factor of the CAMMICE/HIT instrument is $g = 9.1 \times 10^{-3}\mathrm{cm}^2\mathrm{sr}$ (Fritz et al., 1997). The coincidence channels, HID7 and HID8, are largely free of background contamination. The HID5 channel will see pile-up protons in addition to helium ions. The threshold for that channel requires that 0.52 MeV be deposited in the detector in order to trigger the alpha 1 threshold. One can estimate the pileup counts by determining the flux of 260 KeV protons, apply the geometric factor to that flux, and compute an equivalent counting rate, $r$. The pile up count rate for HID5 should be equal to $5 \times 10^{-7} r^2$. So if $r = 1000$ proton counts/sec one should have about 0.5 counts/sec of background in that helium channel. Effects of particle penetration through the backside of the detector would also require penetration through the entire POLAR spacecraft and can reasonably be neglected.

## 2 HELIUM ION DATA BASE

The first half year of the POLAR spacecraft operations afforded an extended period of geomagnetic calm that lasted from the time of the spacecraft launch to October 23, 1996 when a modest geomagnetic storm (as indicated by the provisional $D_{ST}$-index depression to -110 nT) occurred. We thus posses an extensive database on geomagnetically confined helium ions and other ion species for the non-disturbed radiation belts during sunspot minimum conditions. Figure 1 shows a typical trajectory (on July 28, 1996) of the POLAR spacecraft through the Earth's magnetosphere. At that time the orbital plane was close to the dawn-dusk plane, and the trajectory also closely coincided with the nominal plane of the geomagnetic field lines.

An example of the data from the four helium ion detector passbands listed in Table 1 is shown in Figure 2. These data are from July 28, 1996 with the left side panels depicting the observed distribution of the helium ion flux with the $L$-parameter in the geomagnetic dusk sector (MLT ∼ 17 hr) and the right side panels showing the corresponding data from the dawn sector (MLT ∼

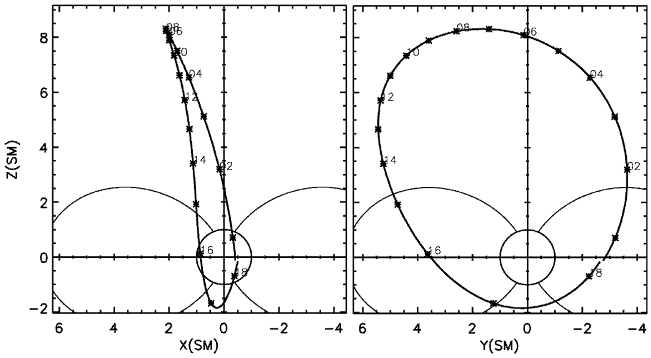


**Fig. 1.** Orbit of the POLAR spacecraft in Solar-Magnetospheric (SM) coordinates during July 28 (day 210) 1996. Numbers on the trajectory trace indicate hour of the day of the spacecraft location.

5 hr). In both cases, the regions of the peak ion fluxes (L ∼ 2.8 to 3.6) were sampled close to the geomagnetic equator. Since the structures of the flux distributions show significant dawn-dusk differences, it is worthwhile to explore whether these are related to temporal variations, or to other more persistent causes in the heart of the Earth's radiation belts.

## 3 LONGITUDINAL QUIET TIME SURVEY

In order to make a comparison between POLAR spacecraft observations made in different magnetic local time sectors, we map the locally observed ion fluxes to the geomagnetic equatorial plane. Previous work suggests that a mapping following an assumed relation:

$$j(\alpha_0) = j(\alpha_0 = \pi/2) \sin^n \alpha_0 \qquad (1)$$

– where $j$ represents differential helium ion flux and $\alpha_0$ is equatorial pitch angle – serves as an approximate descriptor of geomagnetically trapped MeV helium ion anisotropy in the interior of the trapping region. Here the anisotropy parameter, $n$, is empirically determined from the data set. Under this assumption the equatorially mirroring helium ion flux in our energy range is given by:

$$j_0(\alpha_0 = \pi/2) = j(\alpha = \pi/2)(B/B_0)^{n/2} \qquad (2)$$

where subscript-0 denotes equatorial quantities; $j(\alpha = \pi/2)$ is the locally mirroring ion flux at the POLAR spacecraft location where the magnetic induction value is $B$; and $B_0$ is the equatorial magnetic induction on the same geomagnetic field line.

Since we cannot simultaneously measure both $B$ and $B_0$ with one spacecraft, it is necessary to take the $B/B_0$-ratio from a magnetic field model. Well within the interior of the radiation belts and for observations close to the equatorial plane, we used the simple dipole ratio:

$$B/B_0 = \sqrt{4 - 3\cos^2 \lambda}/cos^6 \lambda \qquad (3)$$

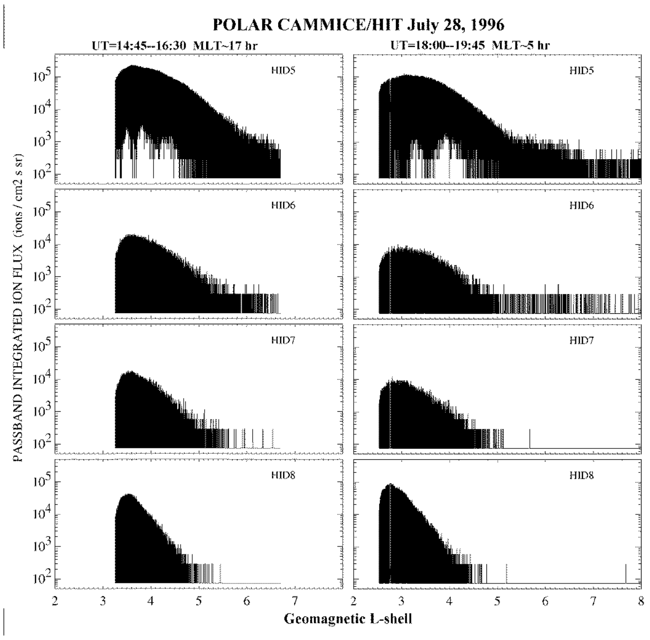


**Fig. 2.** Helium ion flux observed with POLAR in data channels HID5–8 on July 28, 1996. Left panels: UT=14:45–16:30 (dawn sector: MLT$\sim$5 hr); Right panels: UT=18:00–19:45 (dusk sector: MLT$\sim$17 hr). The length of the vertical black bars indicate the spacecraft spin induced variation in the pitch angles (essentially full range) observed.

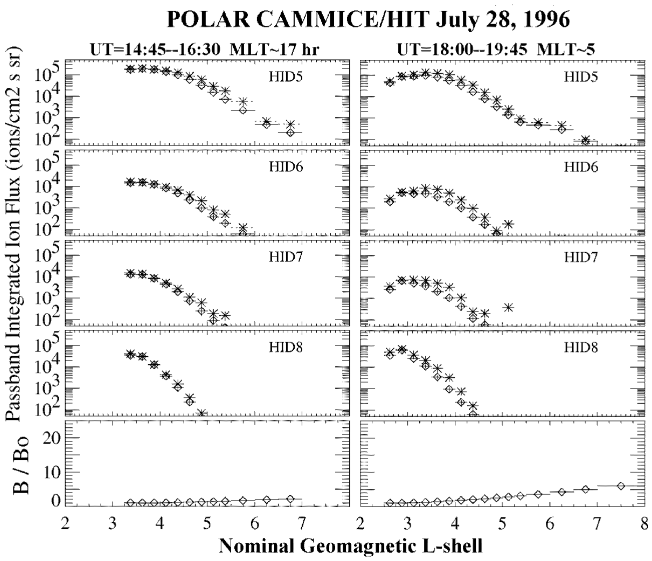


**Fig. 3.** Binned averages of POLAR observed local helium ion flux ($\diamond$) and equatorially mapped flux (*) in helium channels HID5–8. Shown are for UT=14:45–16:30 dusk sector, and for UT=18:00–19:45 dawn sector passes. The bottom panels depict the $B/B_0$-ratios of the orbital spacecraft location.

where $\lambda$ is the instantaneous geomagnetic latitude of the spacecraft. Clearly, this should not be relied on for $L$-parameters outside the geostationary orbit distance or for far off-equatorial locations. We proceeded to determine the anisotropy $n$-values from least-mean-square fits to the local pitch angle distributions. Since the actual equatorial ion pitch angle distributions may differ from the power-sinusoidal-type relationship, such fits may well not be meaningful if the POLAR spacecraft is substantially away from the geomagnetic equator. Based on empirical information from the pitch angle distribution shapes we concluded that the fits must be limited to those near-equatorial POLAR orbital segments where $B/B_0 < 2$.

Figure 3 illustrates the deduced radial profiles of the mapped equatorially mirroring fluxes of helium ion on July 28, 1996. The left side panels show dawn sector fluxes (MLT $\sim$ 5 hr) in the four energy passbands, and the right side panels show the dusk sector results (MLT $\sim$ 17 hr). The data coverage extends from the lowest IGRF 95 ephemeris $L$-parameter observed by POLAR out to $L$=7. One notices that the radial profiles show some apparent dawn-dusk asymmetry both in ion flux magnitude and in the details of the radial structure.

For these two orbital cuts through the radiation belts we also display how the anisotropy index, $n$, was found to vary with the $L$-parameter. The left side panels in Figure 4 show the dawn results and the right side values are for the dusk sector. Again we notice a significant difference between the two local time sectors. In the dawn sector one deduces anisotropy index values that are largely monotonically increasing with decreasing $L$ in to $L$ $\sim$2.5 (the lowest $L$-parameter encountered in that sector). However, in the dusk sector there are indications of non-monotonic $n$-index radial profiles, such that the helium ion pitch angle anisotropy appeared to be largest at $L$ $\sim$5, at least for energies of typically 0.52–1.8 MeV.

These results are not limited to the particular day (July 28, 1996) of the sample data. Similar results were also found for other POLAR spacecraft orbits both during the months preceding and the months following this study. Since large magnetic local time variations at MeV energies were not anticipated so deep within the trapping region during extended geomagnetically quiescent conditions, a more extensive survey of the helium ion azimuthal asymmetry features appeared warranted. The quiet time study was then extended to 40 POLAR spacecraft close-equatorial trajectories during April through October 1996 where the precession of the spacecraft orbital plane (in GSE-coordinates) permitted all magnetic local times to be sampled.

It was first necessary to test whether or not there might be temporal evolutionary trends in the helium ion flux data. If present, such trends might obscure a study of flux variations with magnetic local time based on the slow precession of the POLAR spacecraft over several months. Two characteristic features of the helium ion flux distributions were selected for display: the radial location of the observed helium ion flux peak (typically found near $L$ $\sim$3 in our energy range) and the flux

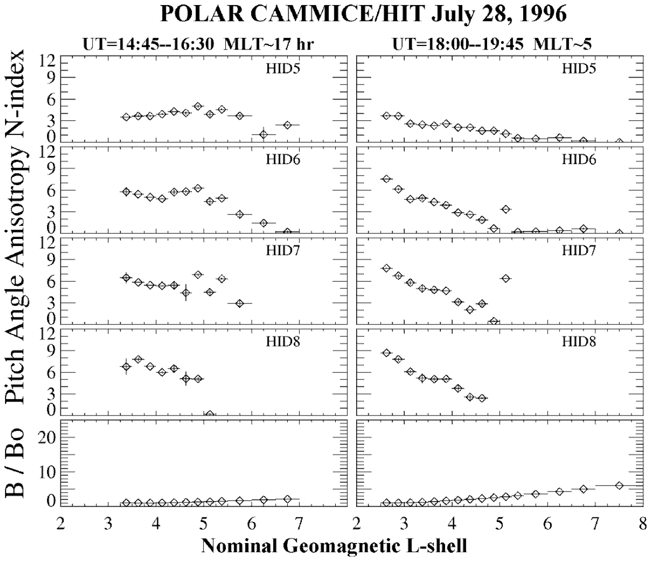


**Fig. 4.** Binned averages of POLAR observed local helium ion pitch angle anisotropy index, $n$, in POLAR data channels HID5–8. For UT=14:45–16:30 a dusk sector pass is depicted, and for UT=18:00–19:45 it is a dawn sector pass. The bottom panels show the spacecraft's proximity of the magnetic equator.

intensity magnitude of that peak. Figure 5 shows the $L$-parameter location radiation belt peak fluxes versus universal time (in decimal day of the year 1996) using one sample data channel (HID7 at 1.8–2.4 MeV), and it is found that there is only a very modest organization of the data and exhibiting almost two $L$-units spread when plotted versus universal time. Our other helium ion data channels show the same features.

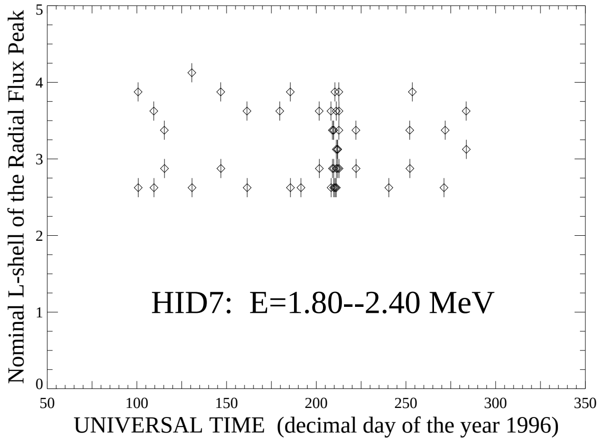


**Fig. 5.** Binned averages of the radial location of the peak in the helium ion differential flux intensity (using $\Delta L$=0.25) plotted versus universal time (decimal day of the year 1996) in POLAR data channel HID7.

Figure 6 shows the corresponding result (also in data channel HID7) for the flux intensities at the radial maxima. Diamonds depict the locally observed fluxes (on orbit segments close to the geomagnetic equator), and asterisks represent the equatorially mapped flux values. Similar to the display in Figure 5, it is here seen that there appears to be a rather limited organization of the data, and we find a spread by about an order of magnitude of the flux peak intensity when plotted versus universal time.

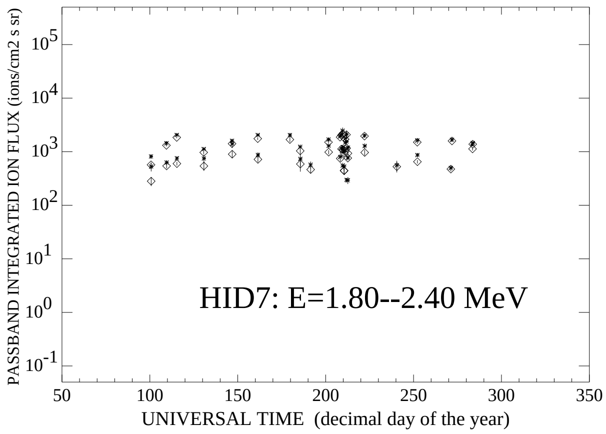


**Fig. 6.** Radial location of the peak in the helium ion differential flux intensity plotted versus universal time (decimal day of the year 1996) in POLAR data channel HID7. Diamonds depict the observed fluxes and asterisks show the equatorially mapped flux intensity.

The outstanding result of this exercise is clearly that there is no systematic temporal trend in the data within the sampling resolution, and we are not observing a helium ion distribution with characteristics that change significantly over the six month period of our data set. Specifically, there is no observed long-term flux decay. This apparent stability feature of the geomagnetically trapped MeV helium ion fluxes permits further analysis based on the overall steady state assumption.

To further study systematic trends in the azimuthal distribution of the helium ion fluxes around the Earth, we plotted two parameters of the distribution, the radial location of the flux peak and the observed flux intensity of that peak versus magnetic local time. The results are depicted in Figure 7 and in Figure 8 using all the four POLAR spacecraft helium ion energy channels HID5–8. The vertical bars in Figure 7 indicate the $L$-parameter range used to bin the data ($\Delta L$=0.25). This figure shows that there exist systematic asymmetries in the energetic helium ion fluxes, and that these are indeed dawn-to-dusk asymmetries that are repeatedly observed, at least when plotted versus the POLAR spacecraft ephemeris parameters. One can see that, compared to an azimuthal average radial location, the MeV helium ion flux peak location in $L$-parameter is shifted inward (towards the Earth) by about half a unit in the dawn sector (MLT$\sim$1–12 hr) and is shifted outward by a similar amount in the dusk sector (MLT$\sim$13–24 hr), leaving a dawn-dusk asymmetry of at least a full unit $L$-parameter wide. This is true in all our four energy

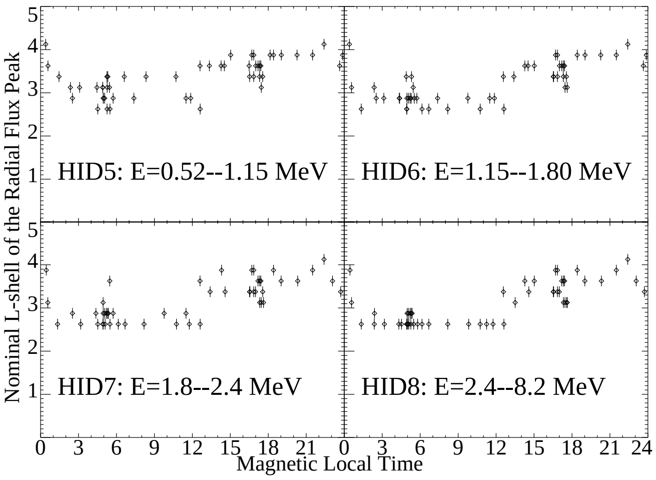


**Fig. 7.** Organization of the $L$-shell location of the radial peak in the helium ion distribution observed by the POLAR spacecraft. Binning into $\Delta L$=0.25 bins was used, and the data are given for channels HID5–8 versus magnetic local time during the geomagnetically quiescent period April – October 1996.

channels.

The peak flux intensities at the radial maximum location appears not to follow quite the same simple dawn-dusk asymmetry pattern. The result in Figure 8 depicts a general increase in flux intensity from very early dawn (MLT∼1–6 hr) towards late dusk (MLT∼18–24 hr). This trend is fairly clear in channels HID5–6 (E ∼ 0.52–1.8 MeV), is weaker in channel HID7 (E∼1.8–2.4 MeV), but appears reversed in channel HID8 (E∼2.4–8.2 MeV). This trend reversal with helium ion energy is suggestive of a possible azimuthal distribution dependence related to distribution function gradients.

## 4 SUMMARY AND EVALUATION OF THE FINDINGS

It has been found that with the POLAR spacecraft ephemeris computed from the IGRF 95 model magnetic field, azimuthal asymmetries appear to be present in quiet time, steady state helium ion distributions at 0.52–8.2 MeV such that in the dawn sector the peak of the radial profiles in MeV helium ion distributions is displaced towards the Earth. The energetic helium ion flux intensities are also higher in this local time sector at E∼0.52–1.8 MeV and lower at E∼2.4–8.2 MeV. Although perfect azimuthal symmetry of geomagnetically confined particles should not be expected around the Earth, the finding that multi-MeV heavy ions seem to exhibit substantial MLT-variations was not fully expected.

It is possible that some of the reported asymmetry results could stem from differences between the real geomagnetic field (as experienced by the trapped particle populations) and the model magnetic field used to com-

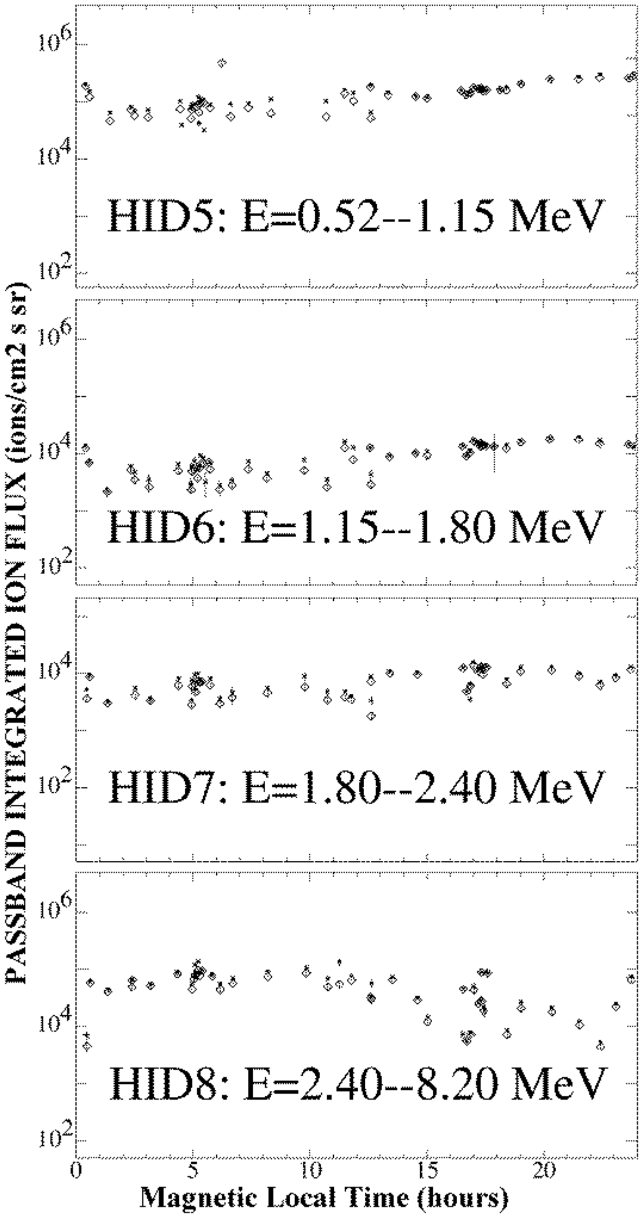


**Fig. 8.** Organization of the radial peak flux intensity in the helium ion distribution observed by the POLAR spacecraft. The data are given for channels HID5–8 versus magnetic local time during the geomagnetically quiescent period April – October 1996.

pute the $L$-parameter, magnetic latitude and longitude. The internal contributions to the geomagnetic field include the effects of an offset dipole, quadrupole, octopole and higher multipole contributions that increase in importance closer to the Earth. Apparent asymmetries resulting from this internal effect should correlate with the planet's rotation, and not predominantly with MLT. Imperfections in the model geomagnetic field used to compute the POLAR ephemeris may be a more significant contributor to MLT asymmetries, and these aspects warrant further exploration.

In addition to possible problems with the spacecraft ephemeris determination, there may also be physical causes of azimuthal asymmetries. The geoelectric field is known to cause $L$-shell splitting effects (e.g., Kivelson and Southwood, 1975a,b; Roederer, 1970; Roederer and Schulz, 1971; Schulz, 1972; Stern, 1971), and the observed azimuthal asymmetry of MeV helium ions may in part be associated with the geoelectric field structure. It is, of course, unlikely that the dawn-dusk electric potential drop (of the order of 50 kV) would have bulk effects on MeV ions. This notwithstanding, some of the observed asymmetries could be the result of the large spectral and spatial gradients found in the trapped ion fluxes combined with the rather modest dawn-dusk geoelectric field, so that even a small shift in the energy spectrum may appear as a significant flux variation seen with instruments of fixed thresholds for detection. Future modeling of these aspects (with and without asymmetric geomagnetic and geoelectric field topology) appears desirable to see if such an interpretation has any merit.

*Acknowledgements.* This work was supported in part by a NASA grant NAG5-2578 to Boston University for data processing and analysis. The authors are grateful to the entire POLAR spacecraft technical management team for data acquisition and routine processing. One of us (WNS) enjoyed the Visiting Scholar guest privileges and hospitality at Boston University during his sabbatical leave from Weber State University. We also want to acknowledge the significant contributions of Bryan Laubscher, Robert Hedges, Rose Vigil, and Gina Lujan on the CAMMICE/HIT sensor system at the Los Alamos National Laboratory; of Rocky Koga, Patricia Lew, Norman Katz, and Bill Crain on the HIT data processing unit at the Aerospace Corporation; and of the administrative support and interest provided by Donald D. Cobb at the Los Alamos National Laboratory.

## References

Chen, J., Guzik, T. G., Sang, Y., Wefel, J. P., and Cooper, J. F., Energetic helium particles trapped in the magnetosphere, *Geophys. Res. Lett.*, *21*, 1583–1586, 1994.

Chen, J., Guzik, T. G., Wefel, J. P., Pyle, K. R., and Cooper, J. F., Energetic helium isotopes trapped in the magnetosphere, *J. Geophys. Res.*, *101*, 24787–24799, 1996.

Cornwall, J. M., Radial diffusion of ionized helium and protons: A probe for magnetospheric dynamics, *J. Geophys. Res.*, *77*, 1756, 1972.

Fritz, T. A. and Spjeldvik, W. N., Observations of energetic radiation belt helium ions at the geomagnetic equator during quiet conditions, *J. Geophys. Res.*, *83*, 2579–2583, 1978.

Fritz, T. A. and Spjeldvik, W. N., Simultaneous quiet time observations of energetic radiation belt protons and helium: The equatorial a/p ratio near 1 MeV, *J. Geophys. Res.*, *84*, 2608–2618, 1979.

Fritz, T. A. and Spjeldvik, W. N., Pitch angle distributions of geomagnetically trapped MeV helium ions during quiet times, *J. Geophys. Res.*, *87*, 5095, 1982.

Fritz, T. A., Daglis, I. A., Livi, S., Sommer, H., Wilken, B., Grande, M., Hall, D. D., Blake, J. B., Fennell, J. F., and Koga, R., The POLAR CAMMICE investigation, Tech. rep., Center for Space Physics, Boston, 1997.

Garcia, H. A. and Spjeldvik, W. N., Anisotropy characteristics of geomagnetically trapped ions, *J. Geophys. Res.*, *90*, 347, 1985.

Kivelson, M. G. and Southwood, D. J., Local time variations of particle flux produced by an electrostatic field in the magnetosphere, *J. Geophys. Res.*, *80*, 56–65, 1975.

Kivelson, M. G. and Southwood, D. J., Note on the electric splitting of drift shells, *J. Geophys. Res.*, *80*, 3525–3527, 1975.

Krimigis, S. M. and Van Allen, J. A., Geomagnetically trapped alpha particles, *J. Geophys. Res.*, *81*, 2275, 1976.

Lemaire, J. F., ed., *Modeling He and H Isotopes in the Radiation Belts*, vol. Geophysical Monograph 97, Washington, D.C., American Geophysical Union, 1996.

Panasyuk, M. I. and Vlasova, N. A., Anisotropy of fluxes of protons and alpha particles with energies greater than 4 MeV in the radiation belts, *Cosmic Res.*, *19*, 52, 1981.

Pugacheva, G. I., Gusev, A. A., Martin, I. M., Spjeldvik, W. N., and Kohno, T., The temporal evolution of 3-9 MeV/nucleon He flux trapped in the magnetosphere, *Geophys. Res. Lett.*, *23*, 2793–2796, 1996.

Reeves, G. D., ed., *Geomagnetically Trapped Energetic Helium Nuclei*, vol. 383, New York, American Institute of Physics, 1996.

Roederer, J. G., *Dynamics of Geomagnetically Trapped Radiation*, Springer Verlag, New York, 1970.

Roederer, J. G. and Schulz, M., Splitting of drift shells by the magnetospheric electric field, *J. Geophys. Res.*, *76*, 1055, 1971.

Schulz, M., Drift shell splitting at arbitrary pitch angle, *J. Geophys. Res.*, *77*, 624, 1972.

Schulz, M. and Lanzerotti, L. J., *Particle Diffusion in the Radiation Belts*, Springer Verlag, New York, 1974.

Sheldon, R. B. and Hamilton, D. C., Ion transport and loss in the Earth's quiet ring current: 1. data and standard model, *J. Geophys. Res.*, *98*, 13491, 1993.

Spjeldvik, W. N., Expected charge states of energetic ions in the magnetosphere, *Space Sci. Rev.*, *23*, 499, 1979.

Spjeldvik, W. N. and Fritz, T. A., Energetic ionized helium in the quiet time radiation belts: Theory and comparison with observation, *J. Geophys. Res.*, *83*, 654, 1978.

Spjeldvik, W. N. and Fritz, T. A., Observations of energetic helium ions in the Earth's radiation belts during a sequence of geomagnetic storms, *J. Geophys. Res.*, *86*, 2317, 1981.

Spjeldvik, W. N. and Fritz, T. A., Experimental determination of geomagnetically trapped heavy ion fluxes, in *Advances in Earth and Planetary Sciences*, edited by R. G. Johnson, vol. 5, Springer Verlag, New York, 1983.

Spjeldvik, W. N. and Rothwell, P. L., The radiation belts, in *Handbook of Geophysics and the Space Environment*, edited by A. S. Jursa, chap. 5, pp. 5.1–5.55, Air Force Systems Command, US Air Force, Washington, D.C., 1985.

Stern, D. P., Shell splitting due to electric fields, *J. Geophys. Res.*, *76*, 7787, 1971.

Tverskoy, B. A., *Dynamics of the Earth's Radiation Belt Region*, vol. Technical Translation, TTF-635, NASA, Washington, D.C., 1971.